ROBOTEX

Automated COVID Screening Entrance Device

Technical Memo

March, 2021

- Prepared for -

Prof: Robert Dony
TA: Amanda Nelson

- Prepared by -

Aarthi Christina Aruliah - 1069952
Layal Alzaydi - 1041786
Lina Shaabo -1053401
Nasiba Alchach - 1072028
Whitney Trinh - 1052299

1.0 Introduction

This paper presents the required calculations and principles needed to create a successful automated COVID screening entrance device which mainly comprises mask detection, body temperature measurement, counting number of people and regulating the customers at the entrance. Each of these components are expanded to provide further understanding to the working of the entire system with the help of sketches, engineering calculations and implementation of codes. The engineers at ROBOTEX have provided necessary assumptions and detailed solutions of this project in this document.

2.0 Problem statement for calculations

The main purpose of the engineering calculations for this design is to ensure a highly effective solution. Engineering calculations are the math behind a design's ability to function properly and efficiently. The team members at ROBOTEX are using knowledge, approaches, and methods from previous engineering courses to determine the limitations and the standards that the design solution must withstand. These include the materials properties and the accuracy of the components required to implement and build the final design.

First, circuits for different sensors are constructed in TinkerCAD using engineering circuits and electronic devices knowledge. Through some circuit analysis and Arduino coding, the sensor that offers a more accurate and appropriate application for our case will be selected. The constructed circuits are designed in TinkerCAD, as shown in **appendix B**. The criteria and the total scores can be found in the decision matrix shown in **appendix D** .

Second, using physics and engineering principles, different dimensions of components are calculated. Since it is essential that the temperature measuring device and the face mask detector are accessible to different demographics, the required calculations are to be conducted to enhance the ability of the camera to detect people of different heights.

Another major problem addressed is the selection of the materials to be selected for the device components. Materials need to pass specific tests in order to be selected. With the help of some material science knowledge, the appropriate materials for the casing of the shell, the glass and the screen will be selected.

3.0 Background Information

The device has many components that work together to ensure that the customers follow the required safety restrictions. When the customer reaches the store entrance, he/she will be faced by (the device). A basic sketch of the device is shown in **Figure 8** in the appendix. It consists of one camera and a thermal sensor placed in a small container, 2 counting sensors, gates, and an automated hand sanitizer box.

The V2 raspberry Camera is used to detect the face mask. It has a Sony IMX219 sensor and an 8-megapixel resolution (compared to the 5-megapixel OmniVision OV5647 sensor of the original camera) (Raspberry Pi n.d.). The image area covered by this camera is 3.68 x 2.76 mm (4.6 mm diagonal)(Asad, 2020). Although many types of cameras can be used in face mask detection, such as CCTV cameras, the v2 raspberry camera has been chosen by the team

because of its tiny size with dimensions of 25mm x 23mm x 9mm and its weight of just 3g(Asad, 2020). Those features make it an easy option to work with on top of its high resolution. Moreover, it uses less power, allows faster bandwidth, and fits within a smaller physical size(Asad, 2020). Overall, RPI camera v2 is a great option for a low-cost outdoor device.

To measure the customers' temperature without any contact, the design team is using the non-contact infrared temperature sensor module (MLX90614). This sensor includes a built-in low noise amplifier, 17-bit ADC, and a powerful DSP module, which is why this sensor's high precision and accuracy (Mnati, Chisab, Al-Rawi, Ali, & Van den Bossche, 2021). The design team chose this sensor model because of its small size, low cost and ease of integration. The sensor's temperature operation is from -40°C to 125°C (Mnati, Chisab, Al-Rawi, Ali, & Van den Bossche, 2021), making this sensor a great option to measure people's body temperature since most thermal cameras do not operate in a cold environment. The infrared sensor works straightforwardly. Any object with a temperature higher than (0)K emits infrared energy measured by an infrared sensor (Mnati, Chisab, Al-Rawi, Ali, & Van den Bossche, 2021). This process involves a lens that focuses on the detector's infrared energy emitted by an object (Mnati, Chisab, Al-Rawi, Ali, & Van den Bossche, 2021). An electrical signal is then created by converting the detected infrared energy; the electrical signal is then passed on to a microcontroller that interprets and displays it as a temperature unit (Mnati, Chisab, Al-Rawi, Ali, & Van den Bossche, 2021). The MLX90614 can detect a wide range of temperatures between -70°C and 380 °C (Mnati, Chisab, Al-Rawi, Ali, & Van den Bossche, 2021).

The thermal sensor will be placed on top of the camera at a distance of about 1 cm apart. Both the camera and the sensor will be attached to a raspberry pi Arduino. Also, the raspberry pi Arduino, the camera, and the sensor will be placed in a small container , and then this container will be attached to a motor which will move the container including the camera up and down depending on the height of the person.

The design team looked at three different motors: brushed and brushless DC motors and the stepper motor. The stepper motor is chosen because it can move in slow, precise and discrete steps which are not available in the other motors(Helen, 2019). The way stepper motor work is by a control system that sends electrical pulses to a driver, and that driver interprets these pulses and sends proportional voltages to the motor (Helen, 2019). This motor has a maximum torque at low speeds, which is less than 2000 rpm (Helen, 2019).

To count the number of people in the store accurately, ultrasonic sensors are used. An ultrasonic sensor emits ultrasonic sound waves to target an object and then converts the reflected sound waves into an electrical signal (Jost, 2019). The ultrasonic sensor consists of two main parts: the transmitter responsible for emitting the sound wave using piezoelectric crystals(Jost, 2019); and the receiver, which records and counts the sound after it has travelled to and back from the targeted object(Jost, 2019). The ultrasonic wave speed is relatively high, which increases the accuracy of this type of sensor (Jost, 2019).

This sensor works based on the distance between the person and the sensor. If the person is closed to the sensor, therefore, the distance between the sensor and the person is less than the assigned distance, then the number of people in the store will be increased by one, and if the distance between the person and the sensor is higher than the assigned distance, then the person is exiting the building so the number of the people in the store will be decreased by one.

4.0 Assumptions

The assumptions required for an effective and accurate design solution in regards to the different components of the design in regards to the circuits, face mask detection, temperature measure technology and the door control are listed in the table below.

Table 1: Engineering Assumptions

#	Assumption	Justification	Source
1	Assume a distance of 178.1 cm between the camera and the person.	This assumption will help develop calculations necessary for the placement of their camera as well as the angles that it is going to adjust itself when scanning people of different heights.	Initiated by ROBOTEX.
2	Assume the design will always have a nearby power source.	No batteries are to be used to provide power to the cameras.	Initiated by ROBOTEX.
3	Assume no black objects are to be worked with (Applicable for IR sensors).	IR sensors do not work with black colored objects, because black fully absorbs the transmitted rays.	(university of Illinois, 2015)
4	Assume only one person is entering and exiting at a time.	This will ensure that the counter results are accurate if the sensor is performing a single detection at a time.	Initiated by ROBOTEX.
5	Assume that people will only be entering from the entrance and exiting from the exit of the store.	This will ensure that the counter results are not affected by any sources of errors, hence people entering and exiting from the wrong door.	Initiated by ROBOTEX.
6	Assume an average height of 171cm for the person being scanned by the temperature measuring and mask detection camera.	This will ensure that the temperature measuring device and the mask detector are accessible to all demographics. The average is based on the average height for men and women in Canada.	(CBC, 2016)

5.0 Material Properties

For the outer casing durability of the design is important. The materials were selected to be of IP66 grade, which ensures the design is weatherproof and can function when exposed to water and dust. All materials that passed this requirement were selected to be further examined. The proposed materials for the casing are 304 or 316L stainless steel, and 5052 or 6061 aluminium. For the gate and camera enclosure, ABS plastic and polycarbonate were considered. From the design matrix, tables 10 in the appendix, 316L stainless steel and polycarbonate were selected. With 316L steel, the environmental impact is the lowest, calculated in appendix table 9, and the corrosion resistance and harness is high so it is durable. In addition, the thermal conductivity is low so overheating of the device won't occur, and the density is on the lower options, allowing the design to be lighter. All these factors make up for the higher price.

For the plastic parts, polycarbonate will be used from table 11 in the appendix. The density is smaller, and it produces smaller carbon emissions.The turnstile gate will be made of this material, to create both an aesthetic look but allow for a more comforting experience for guests. A 4.53 x 2.56 x 1.57 enclosure will be used for the camera (Polycase, n.d.). Polycarbonate will surround the camera to allow for it to function while withstanding weatherproof, dustproof conditions. Using polycarbonate allows for more clarity and transparency, increasing accuracy and resolution.

For the components, an IP66 Shaded LCD screen will be used to display the camera output on a quarter of the screen to assist guests and improve usability (Xenarc, 2012). The remaining space will be used to provide instruction, and can serve as a lighting source for night-time operation if it is a white source. Microprocessors and Arduinos will facilitate the occupancy count. A V2 Raspberry Pi camera, placed at average height and linked to a thermosensor, will determine the temperature and masks verification for customers while being hooked up to a Raspberry pi. A DC motor will move and tilt the camera for patrons who are shorter or taller than that height.

6.0 Engineering Principles, Calculations and Results

6.1 Mask Detection

The main structure of the project as shown in **Figure 9** consists of 5 main files. First, the dataset folder contains the training and testing data, classified into two main subfolders: '*with_mask*' which holds images for individuals wearing masks, '*without_mask*' which contains images for individuals not wearing masks. The dataset consists of 4095 images, 2165 images with mask and 1930 images without a mask. Second, the *'app.py'* file as shown in **Figure 10** Implements the mask detection method. The algorithm can perform face mask detection on images and live stream videos as shown in **Figure 10** implemented using an *'if'* statement depending on the user's input. Third, the *'detect_mask_video.py'* file is responsible for the live video mask detection functionality. Fourth, the *'requirenmnets.txt'* file holds the software frameworks, platforms and libraries required to be installed prior to running the algorithm.

Fifth, the *'train_mask_detector.py'* is responsible for training the convolutional neural network (CNN) using the dataset folders (chandrikadeb7, *chandrikadeb7/face-mask-detection*).

The algorithm detects the percentage of accuracy the customers are wearing the mask (i.e. Completely or partially wearing the mask). The definition for a complete coverage is that the nose and mouth are fully covered. The algorithm was tested by one of the team members as shown in **Figure 11** sections 1,2 and 3. The initial image represents a 100% mask coverage. While the second picture represents a partial coverage in which the detection is 77.60% of no face coverage. As a result, only 22.4% of the mask was detected. The third image represents a 100% of no face coverage.

The Output in **Figure 12** represents the accuracy for both the training and testing sets. The word *'accuracy'* in the figure represents the accuracy of the algorithm tested against the training set. While the *'val_accuracy'* represents the accuracy of the algorithm tested against the testing set**. Table 5** was constructed using the values from **Figure 12.** The '*20 epochs'* from the figure represents the number of times the neural network runs when being trained. Each epoch consists of 120 training images in which the algorithm is going to be trained by. Each epoch consists of 120 images which means that images are being used for training the algorithm which leaves images for testing the algorithm. The data is divided into ~50% for training and into ~50% for testing. CNN manages to get an average accuracy of 97.3% on the training set and 98.8% on the testing as shown in **Table 5.**

6.2 Counter

The counter functionality of the design is implemented using an Arduino Uno microcontroller (*2 Arduino's and 1 LCD sharing I2c*) for counting the number of customers entering and exiting the store and displaying the value on an LCD screen (Team, "Hello world!"). Two microcontrollers are to be placed at the entrance and exit door of the store. A circuit diagram representing the connectivity of the circuit is shown in **Figure 4**. **Table 5** represents the implementation of the Arduino code that is responsible for incrementing the counter when a customer enters the store. The other Arduino will implement a similar algorithm with a change in line 50 in which the counter is to be decremented when a person is detected exiting the store.

The Arduino Uno (*2 Arduino's and 1 LCD sharing I2c*) microcontroller is known as modular circuit boards, which implies that components can be attached to the pins to create a unique circuit. The physics law that governs the functionality of the Arduino are possess Kirchhoff's Current Law which implies that all currents entering a junction equal the current exiting the junction, Kirchhoff's Voltage Law states that the sum of the voltages at every point in a loop is equal to 0, and Ohm's Law which states that the voltage at any given point is product of the current and the resistance (V=IR)(*The actual physics*).

Ultrasonic sensors (*All about ultrasonic sensors & how they work with Arduino* 2020) emit and receive signals in the form of soundwaves. They emit [LAZ4] soundwaves and measure the distance based on the time it takes for the wave to hit the sensor back. The formula used to calculate the distance from the sensor is Distance = ½ T x C, where T = Time in seconds, C = the speed of sound. The speed of sounds However varies depending on the temperature and

humidity, so this calculation must be adjusted accordingly. For example, the speed of sound in dry air at 20 °C = 344 m / s (*Speed of sound in air*).

HC-SR04 Ultrasonic sensors (*HC-SR04 ultrasonic module range finder sensor*) are being used for human detection. They fall within a 3mm accuracy, they detect humans within a range of up to 4m with a 15-degree angle as shown in **Figure 8**. Their working temperature range is from -20 - 80℃ which is compatible with the different seasons of the year. This type of ultrasonic sensor is compatible with the Arduino Uno (*2 Arduino's and 1 LCD sharing I2c*) that is being used as part of the device. The microcontroller operates at a voltage of 5 V, with a high clock speed of 16 MHz and offers 14 digital I/O pins.

6.3 Camera

The camera's height is assumed to be 1.781m based on the average male height in Canada(cbc, 2016). The distance between the camera and the person is also fixed to 1.781m. The camera is perpendicular to the ground, and so is the person. If the person's height is 1.781, the angle of the camera is 0 degrees, as shown in the first case of **Table 3** in the appendix. The camera is placed at an angle of 0 degrees, and it will move down if the person is less than 1.781 m because a sensor will detect the object's height, and a DC motor is attached to the container that holds the camera, which will move the camera up and down. In this case, the height is assumed to be 1.639m which is the average female height in Canada. Using the right triangle properties and the tan inverse to analyze the angle between the reference (0 degrees) and the person's position, as shown in **Table 3** in the appendix. In the last case, when the person's height is higher than 1.781m and the design team assumed the height to be 1.90 m, the same strategy is used to analyze the angle.

7.4 Automated swing barriers

The automated barrier operates with the integration of the outputs from the counter and thermal and mask detection. Depending on these outputs the barrier is controlled. Some of the assumptions made in this design is that the gate must be at least 950mm wide in order for it to be accessible to all (City of Guelph, 2015). Therefore the total width chosen is 1000 mm in this example as this design can be customised accordingly to the store’s entrance size. The calculations provided for the choice of the DC motor is given in **table 8.** These calculations used the following engineering principles like parallel axis theorem, Newton’s second law and full cycle fatigue stresses in determining the optimum DC motor. Fatigue failure is important as there can be seen a repetitive cyclic stress occurring at the steel hinge of the barrier. The corrected endurance limit is estimated.(Norton, n.d.) The assumptions of the design calculations included time to open/close as 2s and the thickness of the barrier to be negligible. The chosen DC motor is of model MM312-2 12V DC from the performance curve. (McMaster Electric, n.d.) In this design the reason for choosing a brushless DC motor is that they are known for holding the torque in stationary in the case of someone kicking the barrier and that they have a smooth operation. (Nundnet, 2020) The arduino controller is used to control the voltage supply to the motor depending on the inputs received from the counter and the mask and temperature detection. The code in **table 6** and the circuit in **figure 14** consists of using an

H-bridge to open and close the barrier by controlling the power provided. Another assumption made in this design was that the barrier is allowed to rotate between 0 and 90 degrees only. In order to accomplish that the servo motor library is used in the code to increment or decrement the angle accordingly until the respective value (0 or 90). The overall important parameters used in the design calculations are listed in **Table 7.**

7.0 Conclusion

To conclude, all technical calculations provided above for the different components of the device justify the accuracy and reliability of the Automated COVID Screening Entrance Device. A thorough mechanical, electrical and software analysis were conducted using assumptions and various physical, electrical and engineering properties such as Kirchaff's Laws , distance, speed and time calculations, Machine learning algorithms, parallel axis theorem, Newton's second law and fatigue analysis were calculated to defend the functionality of the potential design. The accuracy of the face mask detection was calculated using the training and testing data which resulted in a 98% accuracy for the algorithm. Additionally, the angle between the camera and the person is 0 degrees for the average height and the camera can move down with an angle of -4.59 degrees. The camera can move up with an angle of 3.82 degrees when the height of the person is 1.90 m . Moreover, the design proves to be safe to operate under the calculated loads for a long period as the stress generated by the system is under the endurance limit stress . ROBOTEX is committed in designing the finest products so all critical and important calculations were performed and presented to confirm the accuracy, reliability, and effectiveness of the Automated COVID Screening Entrance Device.

8.0 References

2 Arduino's and 1 LCD sharing I2c. (n.d.). Retrieved March 20, 2021, from https://forum.arduino.cc/index.php?topic=503116.0

Adrash S., Mohammed Kaleemuddin S., Binesh B., Ramachandran K.I. (2016). *IOP Conference Series: Materials Science and Engineering.* Performance comparison of Infrared and Ultrasonic sensors for obstacles of different materials in vehicle/ robot navigation applications, *149*(01214). https://iopscience.iop.org/article/10.1088/1757-899X/149/1/012141/pdf

AK Steel. (2021). 316/316L Stainless Steel. AK Steel. https://www.aksteel.com/sites/default/files/2018-01/316316L201706_2.pdf

Asad, S. (2020, July 01). Best Raspberry Pi Cameras. Retrieved March 17, 2021, from https://linuxhint.com/best_raspberry_pi_cameras/

AZoM. (2019, September 04). Stainless steel - Grade 316 (uns s31600). Retrieved March 20, 2021, from https://www.azom.com/article.aspx?ArticleID=863#:~:text=Grade%20316%20is%20the%20standard,crevice%20corrosion%20in%20chloride%20environments.

Baker, A-M., Barry, C.M.F., Cacciatore, A.A., Gastrock, F., Hull, J.L., Izzo, C.P., Kattas, L.N., Kennedy, P., Levin, I.R., Lukaszyk, W.R., Meade, J., Margolis, J., Orroth, S.A., Petrie, E.M., Rotheiser, J.I., Selke, S.E., Shastri, R., Stoughton, P., Wright, R.E. (1999). Modern Plastics Handbook. *Technology Seminars Inc.* https://mmsallaboutmetallurgy.com/wp-content/uploads/2019/08/Modern-Plastics-Handbook.pdf

City of Guelph 2015 Facility Accessibility Design Manual. (2015). Retrieved March 19, 2021, from https://guelph.ca/wp-content/uploads/Guelph_FADM_2015-06-30-FINAL.pdf

CBC. (2016, July 26). Canadians still getting taller, but not as fast as others. CBC News. Retrieved from: https://www.cbc.ca/news/health/height-growth-canada-1.3695398

Chandrika Db7. (n.d.). Chandrikadeb7/face-mask-detection. Retrieved March 20, 2021, from https://github.com/chandrikadeb7/Face-Mask-Detection

Dielectric Manufacturing. (2021). *ABS (Acrylonitrile-Butadiene-Styrene)*. Dielectric Manufacturing. https://dielectricmfg.com/knowledge-base/abs/

Dielectric Manufacturing. (2021). *Lexan® (Polycarbonate).* Dielectric Manufacturing. https://dielectricmfg.com/knowledge-base/lexan/

H. (2019). Choosing the Right Motor for Your Project – DC vs Stepper vs Servo Motors. Retrieved March 19, 2021, from https://www.seeedstudio.com/blog/2019/04/01/choosing-the-right-motor-for-your-project-dc-vs-stepper-vs-servo-motors/

HC-SR04 ultrasonic module range finder sensor. (n.d.). Retrieved March 20, 2021, from https://voltatek.ca/sensors/144-hc-sr04-ultrasonic-module-range-finder.html

Jeremy S Cook Jeremy S. Cook has a BSME from Clemson University, Cook, J., & Jeremy S. Cook has a BSME from Clemson University. (2020, September 29). All about ultrasonic sensors & how they work with Arduino. Retrieved March 20, 2021, from https://www.arrow.com/en/research-and-events/articles/ultrasonic-sensors-how-they-work-and-how-to-use-them-with-arduino

Jorfors, A.E.W., Du, A., Yu, G., Zheng, J., Wang, K. (2020). On the Sustainable Choice of Alloying Elements for Strength of Aluminum-Based Alloys. Sustainability 2020, 12(3). https://doi.org/10.3390/su12031059

Jost, D. (2019, October 7). What is an Ultrasonic Sensor? Retrieved March 18, 2021, from https://www.fierceelectronics.com/sensors/what-ultrasonic-sensor#:~:text=An%20ultrasonic%20sensor%20is%20an,sound%20that%20humans%20can%20hear

KDM Steel. (2021). *IP66 Enclosure.* KDM Steel. https://www.kdmsteel.com/ip66-enclosure/

Learn Robotics. (2019, October 5). *IR Sensors vs. Ultrasonic Sensors: What is the difference.* Retrieved from: https://www.learnrobotics.org/blog/ir-sensor-vs-ultrasonic-sensor/#:~:text=ultrasonic%20sensors%20is%20the%20way,not%20an%20object%20is%20present.

Matmatch. (2021). *AA Standards Grade 5052 H32.* Matmatch. https://matmatch.com/materials/mitf267-aa-standards-grade-5052-h32

McMaster, 78mm-High-Speed-High-Torque-4000rpm-900W-12V-Electric-Dc-Motor. (n.d.). Retrieved March 19, 2021, from https://www.mcmaster-electric.com/78mm-High-Speed-High-Torque-4000rpm-900W-12V-Electric-Dc-Motor-MM312-pd6478510.html

Metalen, S. (2021). *Stainless Steel 304*. Matmatch. https://matmatch.com/materials/salo0057-stainless-steel-304

Mnati, M. J., Chisab, R. F., Al-Rawi, A. M., Ali, A. H., & Van den Bossche, A. (2021). An open-source non-contact thermometer using low-cost electronic components. *HardwareX, 9*. doi:10.1016/j.ohx.2021.e00183

Norton, R. L. (n.d.). MACHINE DESIGN An Integrated Approach (4th ed.). Pearson.

Nundnet. (2020, September 03). Motors used for Turnstiles: Nundnet turnstiles and access controls. Retrieved March 19, 2021, from https://nundnet.com/motors-used-for-turnstiles/

Nyu. (n.d.). Coefficient of friction table. Retrieved March 19, 2021, from https://www.teachengineering.org/content/nyu_/activities/nyu_heavy/nyu_heavy_activity1_coftable.pdf

O. (n.d.). A complete guide to POLYCARBONATE (PC) $neo(document).ready($neo(function () { $neo('.starAvg').rating(); $NEO('.STARAVG').RATING('SELECT', "4"); $neo('.staravg').rating('readonly', TRUE); }));. Retrieved March 19, 2021, from https://omnexus.specialchem.com/selection-guide/polycarbonate-pc-plastic#:~:text=Toughness%20and%20High%20Impact%20Strength,down%20to%20%2D20%C2%B0C.

Polycase (n.d.) *WC-21 Outdoor Enclosure with Clear Cover*.Polycase. https://www.polycase.com/wc-21

Raspberry Pi. (n.d.). Buy a camera Module V2. Retrieved March 20, 2021, from https://www.raspberrypi.org/products/camera-module-v2/

Saevarsdottir, G., Kvande, H., & Welch, B. (2019). Aluminum Production in the Times of Climate Change: The Global Challenge to Reduce the Carbon Footprint and Prevent Carbon Leakage. JOM. 72. doi:10.1007/s11837-019-03918-6.

ScrapMonster. (2021). *Stainless Steel Scrap Prices*. ScrapMonster. https://www.scrapmonster.com/scrap-prices/category/Stainless-Steel/151/1/1

Schweitzer, P.A. (2003). Metallic Materials: Physical, Mechanical, and Corrosion Properties. *Marcel Dekker Inc*. http://fdjpkc.fudan.edu.cn/_upload/article/files/eb/ab/7153debf443bbb5ccdeb1a03f4be/9b511ade-0067-496d-a94c-9f04b57d24be.pdf

Speed of sound in air. (n.d.). Retrieved March 20, 2021, from http://hyperphysics.phy-astr.gsu.edu/hbase/Sound/souspe.html

Team, T. (n.d.). "Hello world!" Retrieved March 20, 2021, from https://www.arduino.cc/en/Tutorial/LibraryExamples/HelloWorld

The actual physics. (n.d.). Retrieved March 20, 2021, from http://ffden-2.phys.uaf.edu/webproj/212_spring_2017/Ryan_Stonebraker/Ryan_Stonebraker/physics.html

The Twenty-Sixth International Training Course. (2016, October 23). *Define Physical Protection System Requirements*. Retrieved from: https://share-ng.sandia.gov/itc/assets/08-intrusion-detection-text.pdf

Toulas, B. (2017, October 25). *6061-T6 Aluminium – The Ultimate Guide.* Engineering Clicks. https://www.engineeringclicks.com/6061-t6-aluminum/

United Performance Materials. (2021). *Stainless 316, 316L, 317, 317L*. United Performance Materials. https://www.upmet.com/sites/default/files/datasheets/316-316l.pdf

University of Illinois at Urbana Champaign. (2015, January 2). *Objects and their colors*. Department of Physics. Retrieved from: https://van.physics.illinois.edu/qa/listing.php?id=28452&t=objects-and-their-colors#:~:text=You%20will%20not%20see%20it,and%20reflect%20the%20light%20back.

Welner, M. (2016, July 18). Gate opener. Retrieved March 19, 2021, from https://forum.arduino.cc/index.php?topic=414908.0

Xenarc. (2021). *12.1" IP67 Rugged Sunlight Readable Optical Bonded Capacitive Touchscreen LCD Display Monitor with HDMI, DVI, VGA & AV Inputs*. Xenarc Technologies.

https://www.xenarc.com/1219GNH-12.1-inch-ip76-ik08-optical-bonded-capacitive-touchscreen-display-monitor-with-hdmi-dvi-vga-av-inputs-hdmi-video-output.html

9.0 Appendices

9.1 Appendix A: Engineering Calculations

Table 2: Canadian Height Calculations
Average male height in Canada = 178.1cm Average female height in Canada = 163.9cm Average height =

Table 3: Camera Angle Calculations
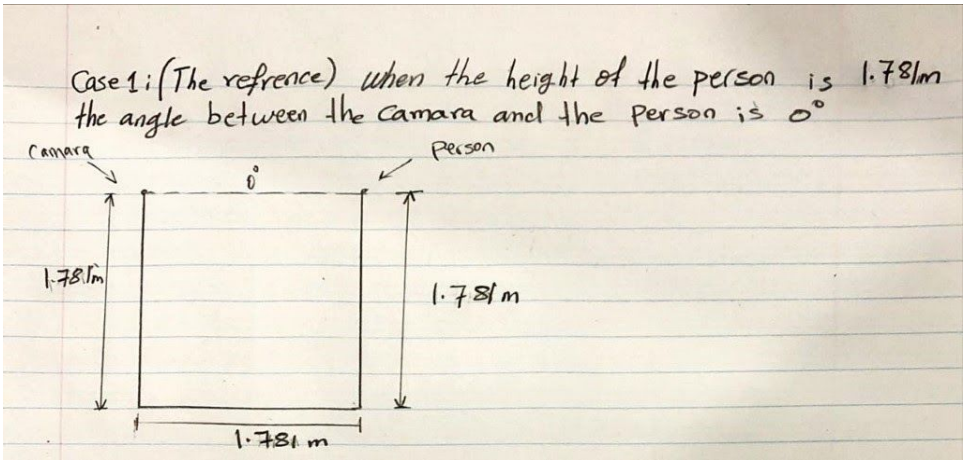   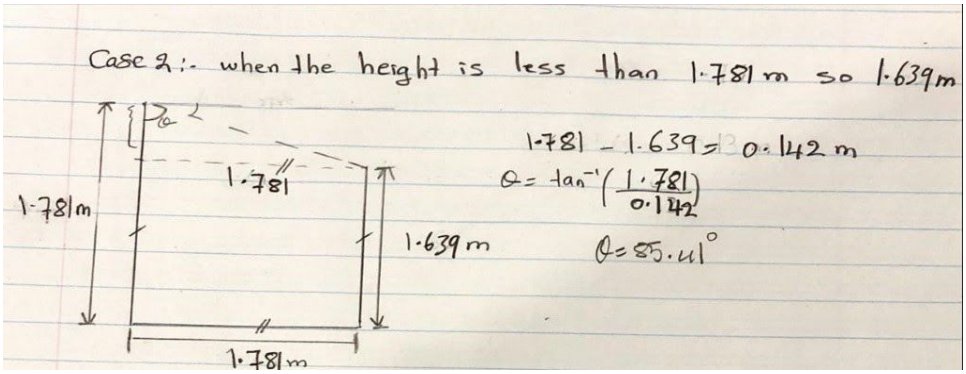

Case 3:- when the height is higher than 1.781 m so 1.90 m

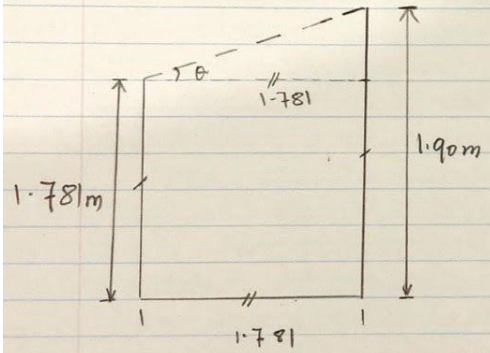

$1.90 - 1.781 = 0.119$

$\theta = \tan^{-1}\left(\frac{0.119}{1.781}\right)$

$\theta = 3.823^{\circ}$

Table 4: Camera angle calculations used as a reference

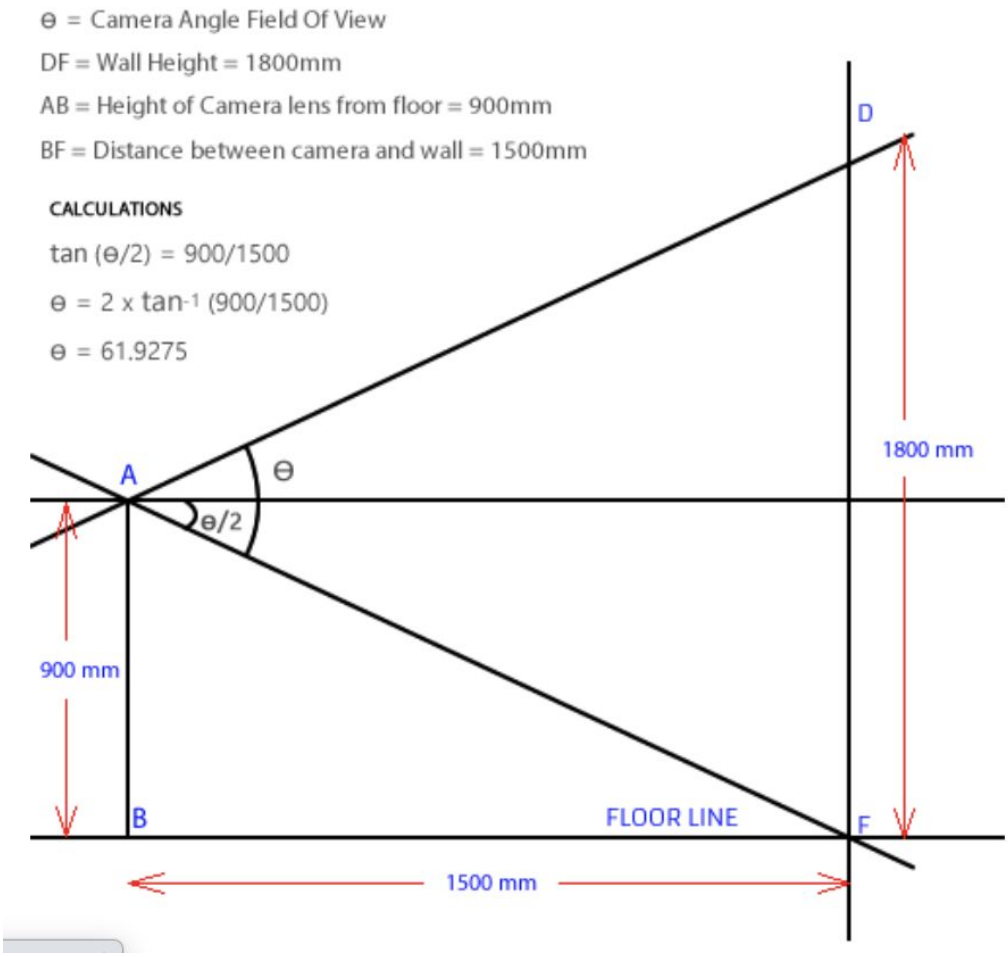

9.2 Appendix B: Constructed Circuits for Proximity Sensors

Figure 1: Constructed Circuit for IR Sensor (Arduino Visitors Counter | Automated Light

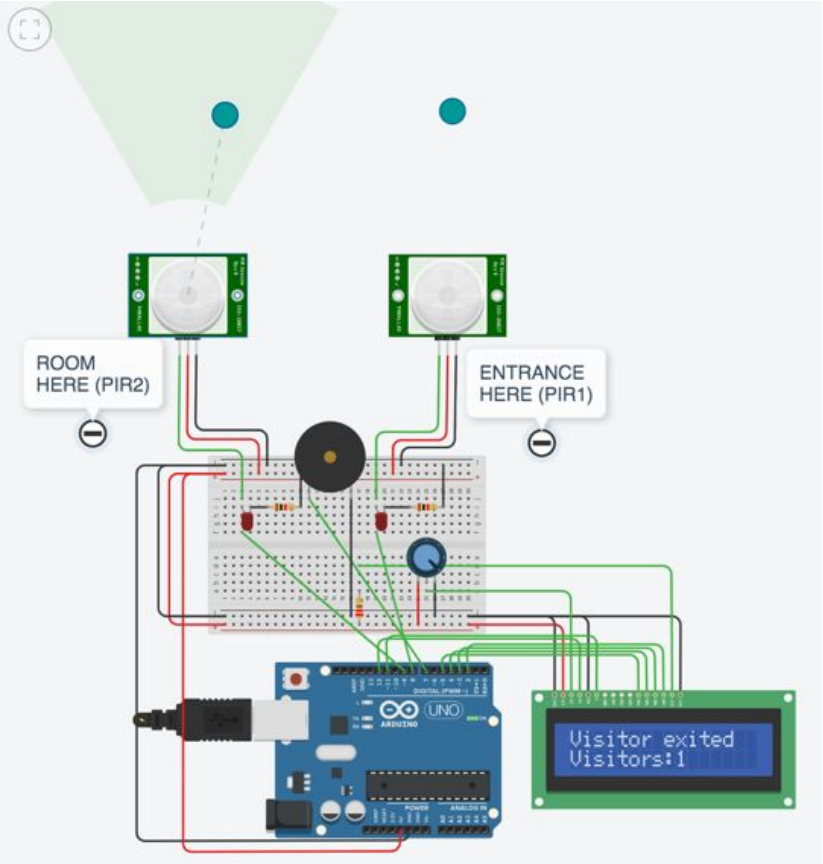

Figure 2: TinkerCAD Circuit representing the Arduino connectivity with the Ultrasonic sensors

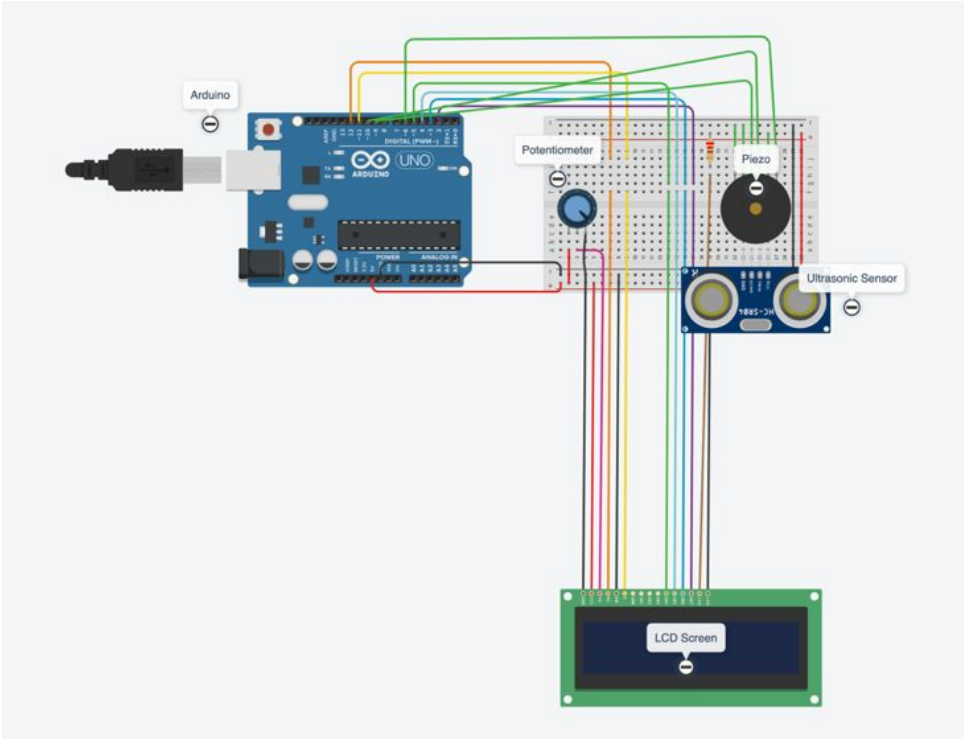

Figure 3: TinkerCAD with people entering the store simulation

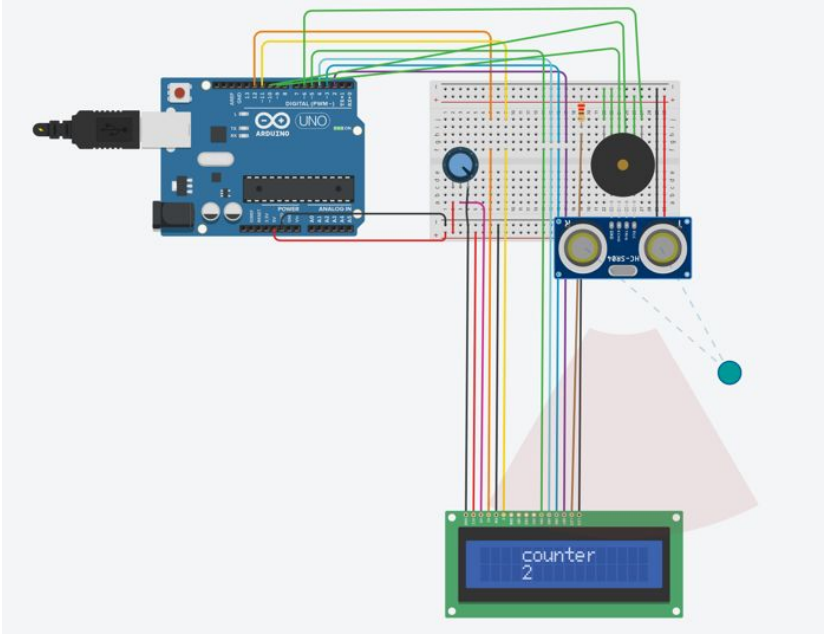

Figure 4: Circuit diagram representing the actual implementation of the Arduinos with the LCD screen

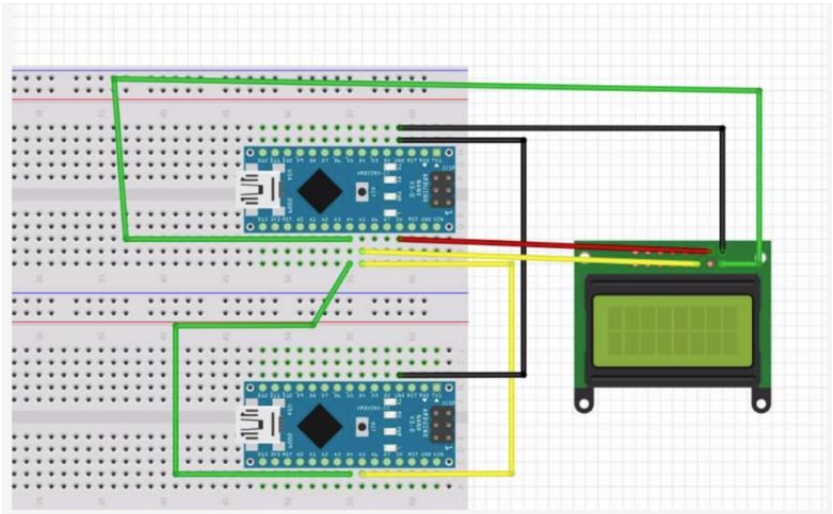

9.3 Appendix C: Automated Swing Barrier Block Diagram

***Figure 5: Block Diagram* for DC motor control process**

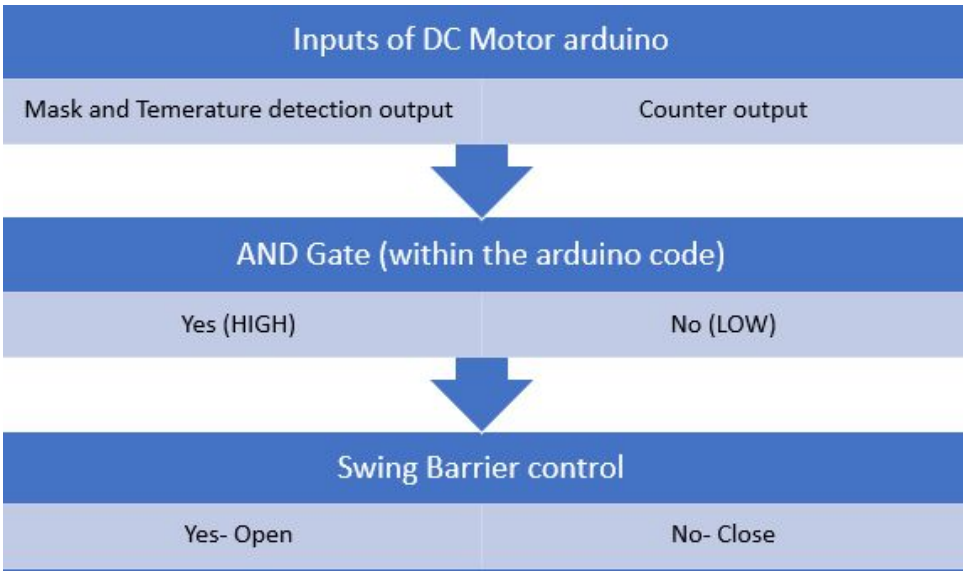

9.4 Appendix D: Decision Matrix

Table 5: Engineering Decision Matrix for IR Sensor VS. Ultrasonic Sensor

		Type of Sensor		Justification
#	**Criterion**	**Infrared Sensor**	**Ultrasonic Sensor**	
1	**Effectiveness**	1	1	Both sensors are widely used for counting purposes and both imply sufficient results (IOP Conference Series: Materials Science and Engineering, 2016)

2	**Simplicity**	1	1	Constructed circuits in TinkerCAD imply that both sensors are simple to build.
3	**Cost-effectiveness**	1	0	Infrared sensors are widely used to their low cost [].
4	**Accuracy**	0	1	Ultrasonic sensors are more reliable for numerical representation of distance and proximity applications due to their high accuracy (Learn Robotics, 2019)
5	**Location Flexibility**	0	1	Ultrasonic Sensors are completely insensitive to light, dirt, dust, and high-moisture environments. The functionality of Infrared sensors can be impacted by the sunlight if used outdoors (The Twenty-Sixth International Training Course, 2016).
Total Points		**3**	**4**	

9.5 Appendix E: Technical Sketches

Figure 6: Zoomed in Technical Sketch of the Design for dimensions Dimensions

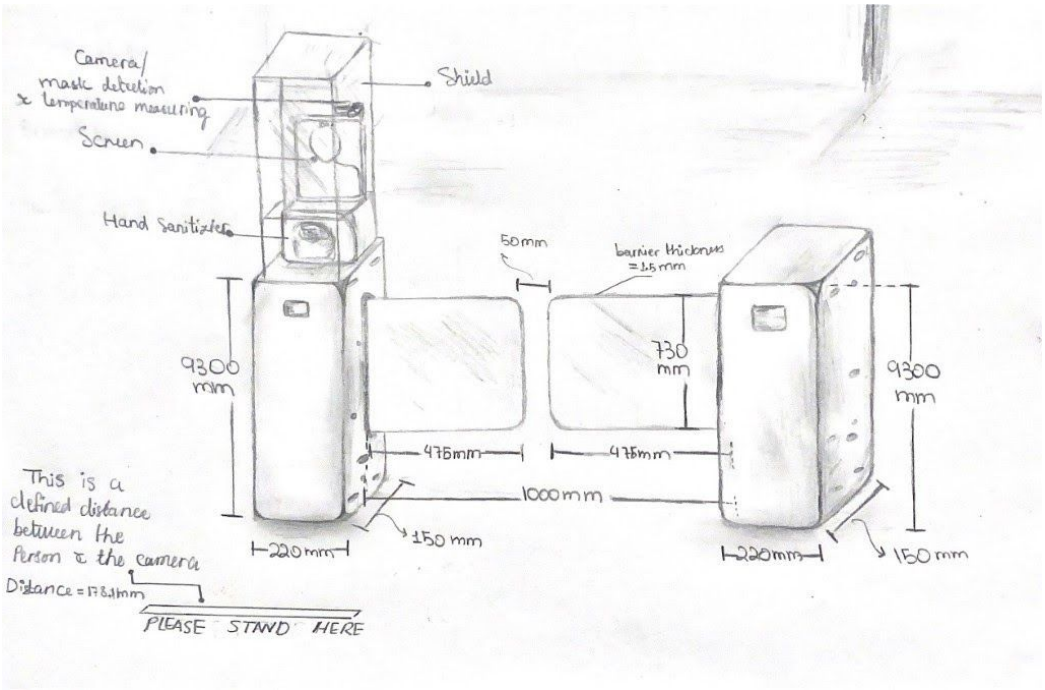

Figure 7: Overall Sketch of Design

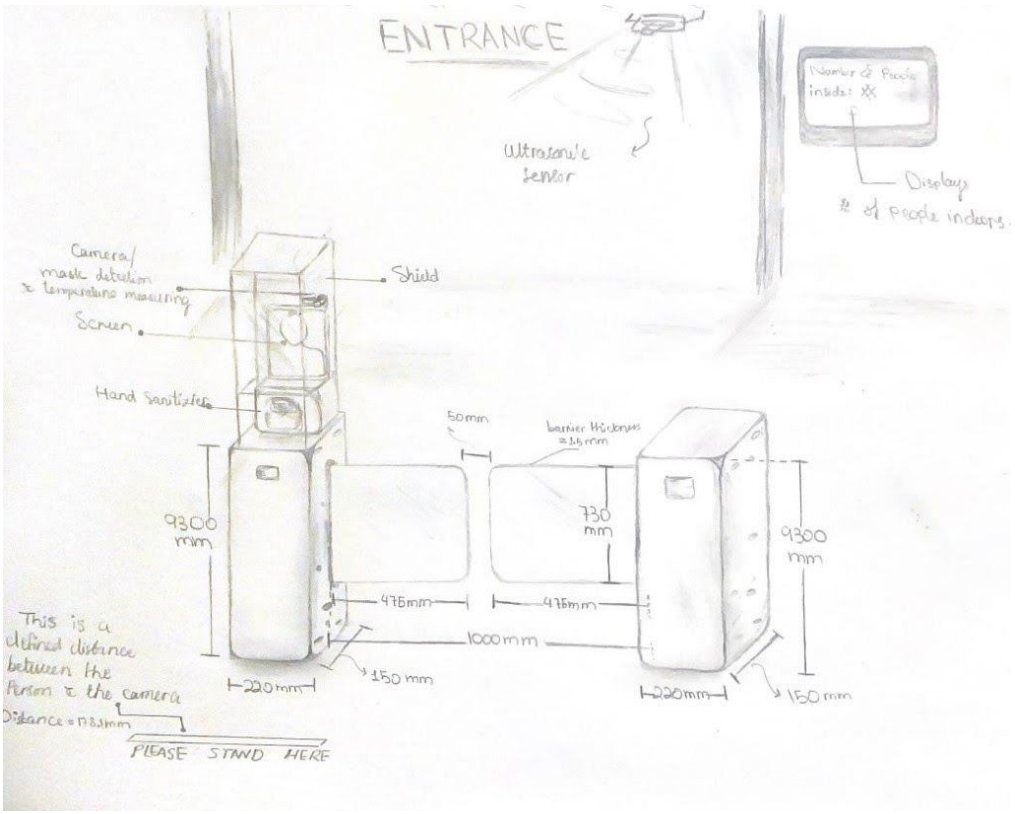

Figure 8: Ultrasonic Sensor with Beam angle measurement range

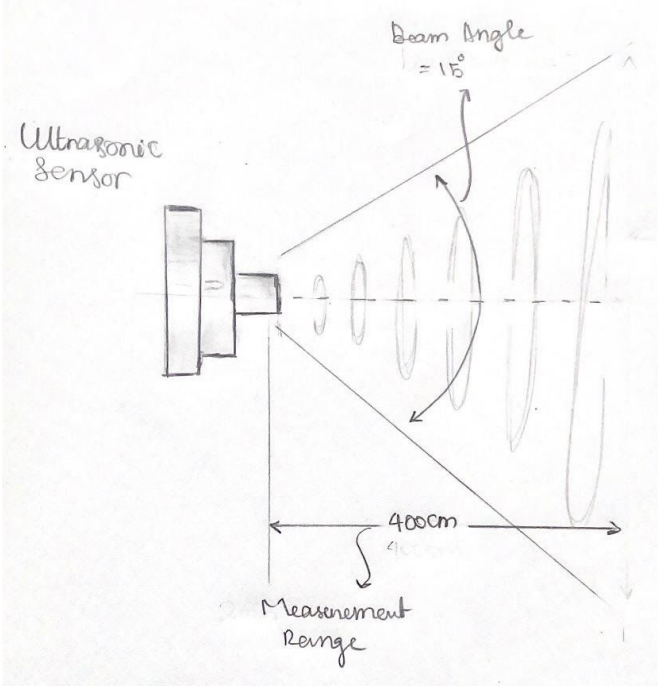

9.6 Appendix F: Software Implementations

Figure 9: Mask Detection project Structure

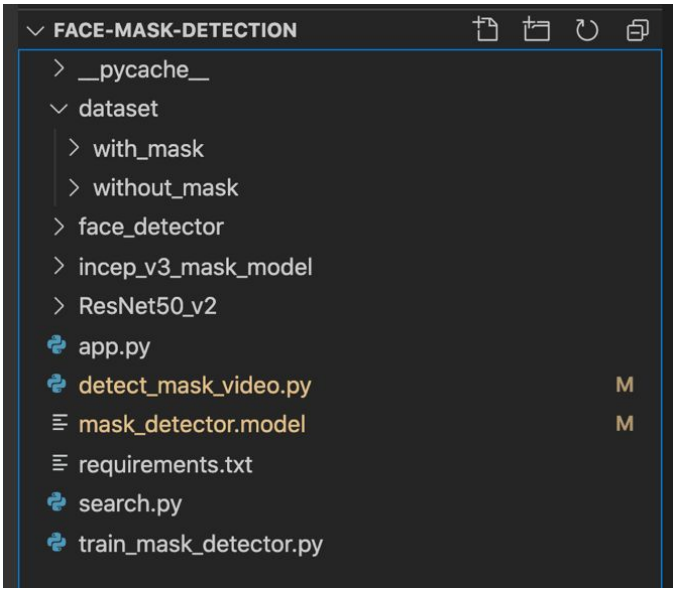

Figure 10: app.py mask detection method

app.py

```
95
96  def mask_detection():
97      local_css("css/styles.css")
98      st.markdown('<h1 align="center">😷 Face Mask Detection</h1>', unsafe_allow_html=True)
99      activities = ["Image", "Webcam"]
100     st.set_option('deprecation.showfileUploaderEncoding', False)
101     st.sidebar.markdown("# Mask Detection on?")
102     choice = st.sidebar.selectbox("Choose among the given options:", activities)
103
104     if choice == 'Image':
105         st.markdown('<h2 align="center">Detection on Image</h2>', unsafe_allow_html=True)
106         st.markdown("### Upload your image here ⬇")
107         image_file = st.file_uploader("", type=['jpg'])  # upload image
108         if image_file is not None:
109             our_image = Image.open(image_file)  # making compatible to PIL
110             im = our_image.save('./images/out.jpg')
111             saved_image = st.image(image_file, caption='', use_column_width=True)
112             st.markdown('<h3 align="center">Image uploaded successfully!</h3>', unsafe_allow_html
113             if st.button('Process'):
114                 st.image(RGB_img, use_column_width=True)
115
116     if choice == 'Webcam':
117         st.markdown('<h2 align="center">Detection on Webcam</h2>', unsafe_allow_html=True)
118         st.markdown('<h3 align="center">This feature will be available soon!</h3>', unsafe_allow_
119 mask_detection()
120
```

Figure 11: Real time face mask detection

Figure 11.1: 100% Mask	**Figure 11.2: Not fully wearing the mask**	**gure 11.3: 100% No mask**
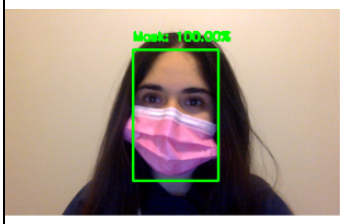	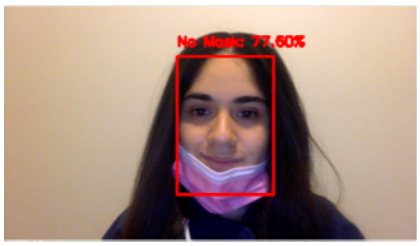	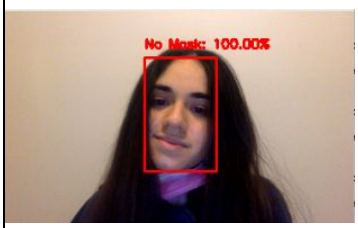

Figure 12: Mask detection CNN (Convolutional Neural Network) algorithm accuracy

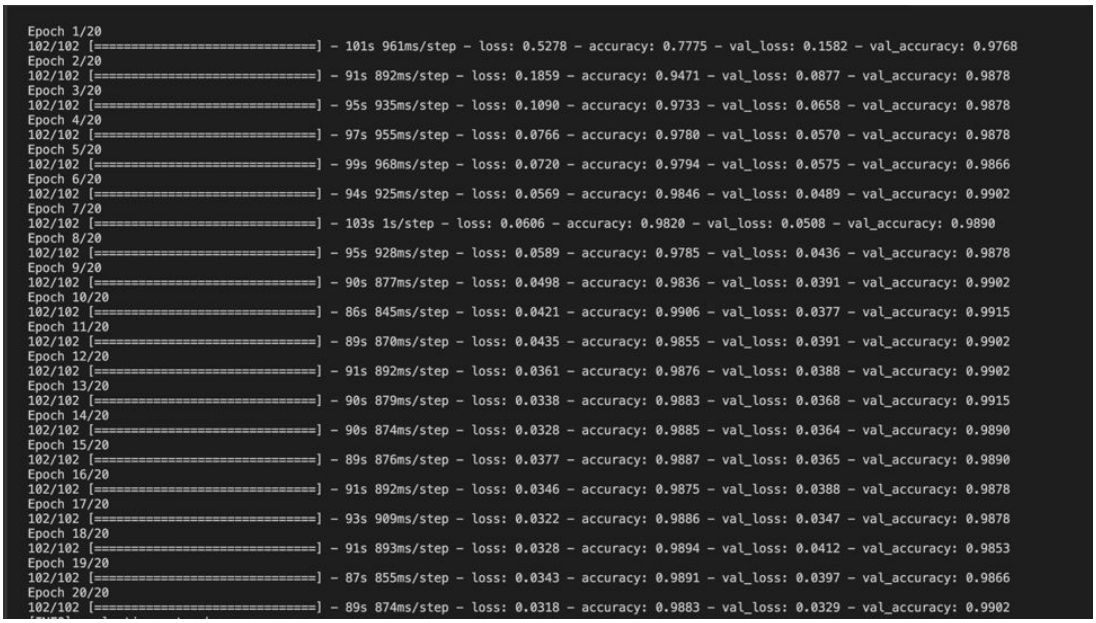

Table 5: Training VS Testing average accuracies

Echo	accuracy	val_accuracy
1	0.7775	0.9768
2	0.9471	0.9878
3	0.9733	0.9878
4	0.978	0.9878
5	0.9794	0.9866
6	0.9846	0.9902
7	0.982	0.989
8	0.9785	0.9878
9	0.9836	0.9902

10	0.9906	0.9915
11	0.9855	0.9902
12	0.9876	0.9902
13	0.9883	0.9915
14	0.9885	0.989
15	0.9887	0.989
16	0.9875	0.9878
17	0.9886	0.9878
18	0.9894	0.9853
19	0.9891	0.9866
20	0.9883	0.9902
Mean	**0.972805**	**0.988155**
Mean as percentage (%)	**97.2805**	**98.8155**

Figure 13: Arduino Code for Motion detection and updating LCD Screen

```
//Ultrasonic
#include <LiquidCrystal.h>
int trigPin = 10;
int echoPin = 9;

int val = 0; // variable for reading the pin status
int counter = 0;
int currentState = 0;
int previousState = 0;

LiquidCrystal lcd(12, 11, 5, 4, 3, 2);

void setup()
{

  lcd.begin(16, 2);
  lcd.setCursor(4, 0);
  lcd.print("counter");
  pinMode(trigPin, OUTPUT);
  pinMode(echoPin, INPUT);

}

void loop()
{

  lcd.setCursor(0, 1);

  long duration, distance ;
 digitalWrite(trigPin, LOW);
 delayMicroseconds(2);
 digitalWrite(trigPin, HIGH);
 delayMicroseconds(10);
 digitalWrite(trigPin, LOW);
 duration = pulseIn(echoPin, HIGH);
 distance = (duration/2) / 29.1;
 if (distance <= 157)
 {
  currentState = 1;
 }
 else
 {
  currentState = 0;
 }

 if(currentState != previousState)
 {
   if(currentState == 1)
   {
     counter = counter + 1;
     lcd.setCursor(4,1);
     lcd.print(counter);
     delay(500);
    }
  }
}
```

9.7.3 Appendix G: Automated Swing Barrier

Figure 14: Automated Swing Barrier

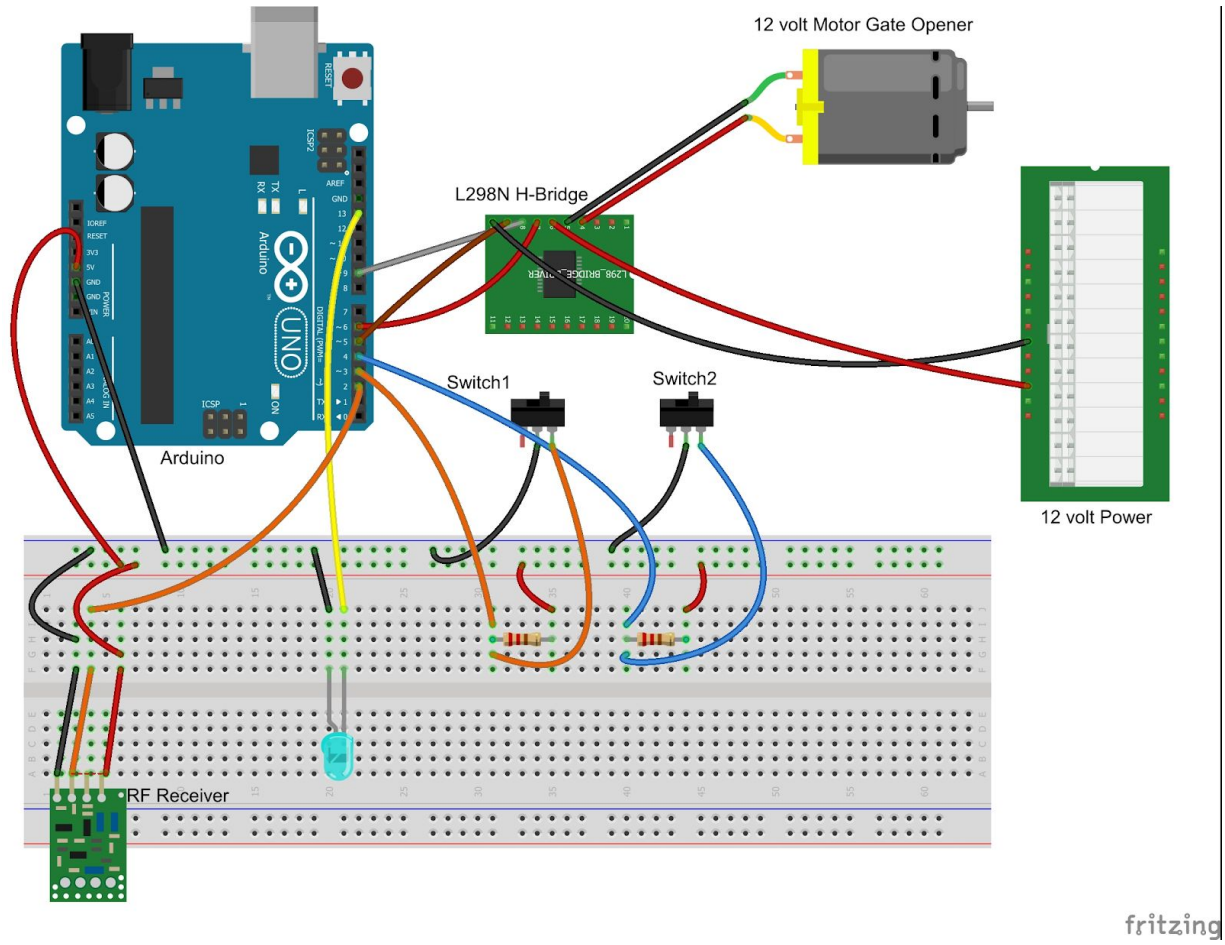

Table 6: Arduino Code for DC motor control

```
#include xxxx                //Servo Library
Servo serv_test;      //initializing servo motor

int angle =0;

int pwm = 9;
int firstinputpin = 2;
int secondinputpin = 3;
```

```
int openNow = 6;
int closeNow = 5;
int firststatus = LOW;
int secondstatus = LOW;
int ledPin = 13;


void setup()
{
 Serial.begin(9600);
 servo_test.attach(8); // attach signal pin of motor to pin 8
pinMode(firstinputpin, INPUT); // takes mask and temperature detection output as an input (switch
1)
 pinMode(secondinputpin, INPUT); // takes counter output as input (switch 2)
 pinMode(openNow, OUTPUT); // send openGate command to H-bridge
 pinMode(closeNow, OUTPUT); // send closeGate command to H-bridge
 pinMode(pwm, OUTPUT); // send speed command to H-bridge
 analogWrite(pwm, 0);  //make sure H-Bridge is off
 pinMode(ledPin, OUTPUT);  //setup our status LED



 if(firststatus == LOW || secondstatus == LOW) //if one of the inputs don't allow for the customer
to enter
 {
  delay(2000); //delay for 2 seconds
  analogWrite(pwm, 0);     // Stops motor
  Serial.println("Please Scan");
 }
 }

void loop() {

 firststatus = digitalRead(firstinputpin);  // for reading in the input 1
 secondstatus = digitalRead(secondinputpin); // for reading in the input 2

    if(firststatus == HIGH && secondstatus == HIGH) //both counter and screening test must be
passed
 {
      openGate();   //sends loop to "openGate" module
```

```
 }
 else
 {    //sends loop to "closeGate" module
       closeGate();
 }

}

void openGate()
{    // opens gate till the gate meets open limit switch
  Serial.println("Welcome!");
  digitalWrite(ledPin, HIGH); //Green light 'ON'!
  digitalWrite(openNow, HIGH);
  analogWrite(pwm, 255); //maximum power

  for(angle =0; angle< 90 ; angle += 1) //move from 0 to 90 degrees)
  {
    servo_test.write(angle);          // to rotate to that specified angle)
    delay(22.222); // to obtain a total opening time of 2s
   }
 while (firststatus == HIGH && secondstatus == HIGH)  {
  delay(2000); //kept open for 2s
  firststatus = digitalRead(firstinputpin);  // for reading in the input 1
 secondstatus = digitalRead(secondinputpin); // for reading in the input 2

 }
 digitalWrite(openNow, LOW);
  analogWrite(pwm, 0);
  digitalWrite(ledPin, LOW);
}

void closeGate()  {     // opens gate till the gate meets close limit switch
 Serial.println("Please Scan");    // for debugging purposes
 digitalWrite(ledPin, HIGH);
 digitalWrite(closeNow, HIGH);
 analogWrite(pwm, 245);
for(angle =90 ; angle>=1 ; angle -= 1) //move back from 90 to 0 degrees)
  {
    servo_test.write(angle);          // to rotate to that specified angle)
    delay(22.222); // to obtain a total opening time of 2s
```

```
  }

 while (firststatus == LOW || secondstatus == LOW)  {
  delay(50);
firststatus = digitalRead(firstinputpin);  // for reading in the input 1
 secondstatus = digitalRead(secondinputpin); // for reading in the input 2
}
 digitalWrite(closeNow, LOW);
 analogWrite(pwm, 0);
 digitalWrite(ledPin, LOW);

}
}
```

Table 7: Parameter used in design calculations	
ρ (barrier)	1.2 g/cm3 (Omnexus, n.d.)
Height (H), barrier	730 mm
Width (W), barrier	475 mm
Thickness(t), barrier	1.5 mm
Full/ Maximum swing angle	0.5*pi* or 90 degrees
S_{ut} , 316L stainless steel	485 MPa (AZoM, 2019)
Time (open/close)	2s
Tau_f, kinetic friction (steel on steel)	0.62 (nyu, n.d.)

Table 8 Calculations pertaining to DC motor design and checking for fatigue failure

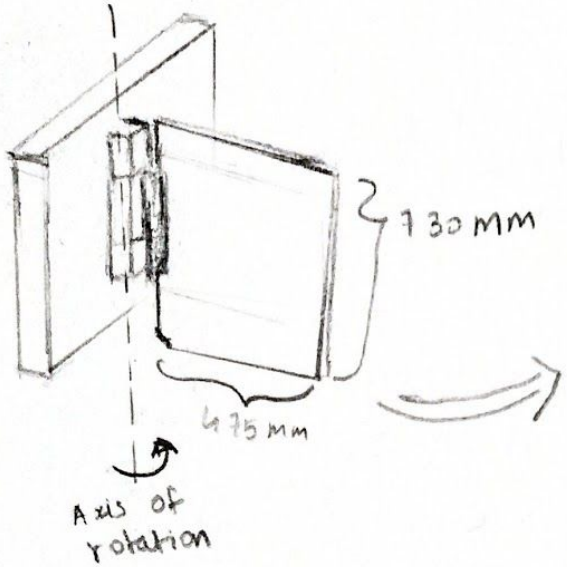

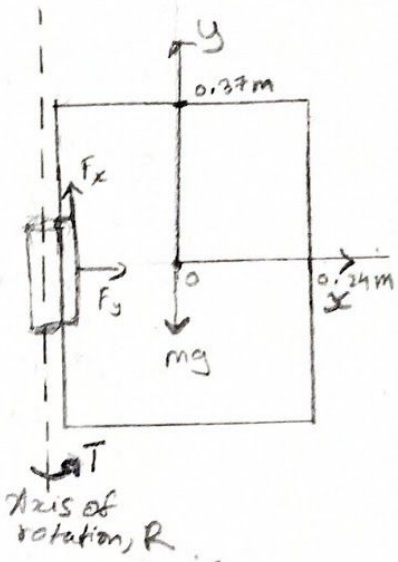

$I_R = I_y + md^2$ → From Parallel Axis Theorem

$m = \forall \times \rho = 475 \times 730 \times 1.5 \times 1.20 \times 10^{-3}$ [g]

$= 0.624$ kg

$I_y = \left(\frac{m}{12}\right) \times b^2 = \frac{0.624}{12} \times (475 \times 10^{-3})^2 = 0.025 \text{ kg m}^2$

$\Rightarrow I_R = 0.025 + (0.624 \times (347.5 \times 10^{-3})^2)$

$= 0.0469 \text{ kg m}^2$

Law of Conservation of Energy:

$$\frac{1}{2} I (\omega_t^2 - \omega_{t'}^2) = \tau_f (\theta_t - \theta_{t'})$$

where, τ_f - kinetic friction, for Stainless steel on stainless steel = 0.62

$\therefore \theta_t = \frac{\pi}{2}$ $\theta_{t'} = 0$ $\omega_{t'} = 0$

$$\therefore \omega_t = \sqrt{\frac{2}{I} \tau_f (\theta_t - \theta_{t'})} = 6.44 \text{ rad/s}$$

$$\therefore n = \frac{60}{2\pi} \times \omega_t = 61.52 \text{ rpm}$$

From Newton's 2nd Law: $\sum T = I\ddot{\theta}$

$\therefore T_{motor}(t) - mgw\sin(\theta(t)) = I\ddot{\theta}(t)$

Assuming the desired target where $t = 2s$ &

$\theta(t) = 0.5\pi \quad \ddot{\theta}(2) \simeq 0$

$\therefore T_{motor} = 0.624 \times 9.81 \times 475 \times 10^{-3} \times \sin(0.5\pi)$

$= 2.91\ N.m$

Based on the Performance Curve choosing model HM312-2 12V-DC Motor with gear ratio Ratio $\simeq 1:36$

FATIGUE ANALYSIS:

$S_{ut} = 485\ MPa < 200\ ksi$ (for 316L Stainless Steel)

$\therefore S_e' = 0.5\ S_{ut}$

$= 242.5\ MPa$

$\frac{I}{J} = \frac{\tau}{Y}$

$\tau_{max} = \frac{3.3 \times 39 \times 10^{-3}}{\frac{\pi \times (78 \times 10^{-3})^4}{32}} = 35.42\ kPa$

$S_e = C_{load} C_{size} C_{surf} C_{temp} C_{reliability} S_e'$

$\Rightarrow C_{load} = 1$ (Bending) $\quad C_{size} = 1.198\, d^{-0.097} = 0.79$

$C_{surf} = 4.51 (S_{ut})^{-0.265}$ (∵ Cold-rolled)

$C_{surf} = 0.88$

$C_{temp} = 1$ for $T \leq 450°C$

$C_{reliab} = 0.897$ for 90% Reliability

$\therefore S_e = 151.22\ MPa$

FATIGUE LIMIT Stress, $S_e \gg \tau_{max}$.

Table 9: Calculations for CO2 Emissions for metal materials. Any compositions below 0.001% were assumed to be negligible

Material	Composition (%) (Jorfors et al, 2020)	CO2 Emission for chemical (kg CO2/kg i) (Jorfors et al, 2020)	Calculation for emission
Aluminium 5052	25 Mg	44.2	0.025*44.2+0.0025*20+0.9725*1.45e4=1.4102e4
	0.25 Cr	20	
	97.25 Al	14.5 tons * 1000kg/1ton= 1.45e4 (Saevarsdottir et al, 2019)	
Aluminium 6061	0.6 Si	4.78	0.006*4.78+0.0075*4.78+0.2*20+0.105*11.2+0.7*2.18=1.42e4
	0.28 Cu	3.44	
	1 Mg	44.2	
	0.2 Cr	20	
	97.92 Al	1.45e4	
Stainless Steel 304	2 Mn	3.8	0.02*3.8+0.0075*4.78+0.2*20+0.105*11.2+0.7*2.18=6.81
	0.75 Si	4.78	
	20 Cr	20	
	10.5 Ni	11.2	
	70 Fe	2.18	
Stainless Steel 316	2 Mn	3.8	0.02*3.8+0.0075*4.78+0.16*20+0.1*11.2+0.69645*2.18=5.94
	0.75 Si	4.78	
	16 Cr	20	
	10 Ni	11.2	

	69.045 Fe	2.18	

Table 10: Decision matrix of metal casing material

Criteria	Material Properties				Weighting	Ranking			
	304 Stainless Steel	5052-O Aluminium	6061 Aluminium	316L Stainless Steel		304 Stainless Steel	5052-O Aluminium	6061 Aluminium	316L Stainless Steel
Environmental impact (kg CO2/kg i) (Refer to table 9)	6.81	1.41x 10^4	1.42x 10^4	5.94	20	3	2	1	4
Average Cost ($/lb)(Scrap Monster, 2021)	0.56	0.76	0.49	0.76	30	2	1	3	1
Corrosion resistant (Schweitzer, 2003)	Med	Med	High	High	5	1	1	2	2
Thermal Conductivity (Btu/hr/ft2/F) (Schweitzer, 2003)	9.4	960	900	9.3	5	3	1	2	4
Hardness	215 (Metalen, 2021)	60-61 (Matmatch, 2021)	60 (Toulas, 2017)	215 (AK Steel)	10	2	1	1	2
Density (lb/in3) (Schweitzer, 2003)	0.29lb/in3	0.097 lb/in3	0.098lb/in3	0.286 lb/in3	15	1	4	3	2
Availability in Canadian	3	0	4	3	10	2	1	3	2

Stores [cite]									
Weighted Total					100	21	16.5	22.5	23

Table 11: Decision Matrix of Plastic related components

Criteria	Material Properties		Weighing	Ranking	
	ABS thermoplastic	Polycarbonate		ABS thermoplastic	Polycarbonate
Environmental impact (kg CO2/kg i) (Dielectric Manufacturing, 2021a;2021b)	9.1e7 - 1.02e8	4.27 - 4.71	20	1	2
Average Cost ($/in3) (Baker et. al, 1999)	0.032	0.073	30	2	1
Transparency/Clarity (Dielectric Manufacturing, 2021a;2021b)	med	high	10	1	2
Thermal Conductivity (Baker et. al, 1999)	lower	low	10	1	2
Availability in Canadian Stores [cite]	10	13	5	1	2
Density (g/cm3) (Baker et. al, 1999)	1.2	1.18	15	1	2

Weighted Total			100	13	17